Original Research

Spider peptide toxin lycosin-I induces apoptosis and inhibits migration of prostate cancer cells

Hongwei Shen[1], Yuan Xie[2], Senlin Ye[3], Kancheng He[3], Lu Yi[3] and Rongrong Cui[4]

[1]Centralab of the Second Xiangya Hospital of Central South University, Changsha 410011, China; [2]Xiangya School of Medicine, Central South University, Changsha 410200, Hunan, China; [3]Department of Urology, The Second Xiangya Hospital of Central South University, Changsha 410011, China; [4]Institute of Metabolism and Endocrinology, The Second XiangYa Hospital of Central South University, Changsha 410011, China

Corresponding authors: Lu Yi. Email: yilu9999@csu.edu.cn; Rongrong Cui. Email: rongrongcui@csu.edu.cn

Impact statement

The spider peptide toxin has become an important research topic. These toxins are molecularly diverse and some display not only a strong antibacterial effect but also exhibit significant inhibition of tumor growth and promote tumor cell apoptosis. Inspired by previous studies, the present study aims to investigate the effects of different concentrations of lycosin-I on the invasiveness and apoptosis of human prostate cancer cells. The findings provide favorable evidence for further study of the molecular diversity of spider toxins.

Abstract

Spider toxins are molecularly diverse and some display not only a strong antibacterial effect but also exhibit significant inhibition of tumor growth and promote tumor cell apoptosis. The aim of the present investigation was to explore different antitumor effects of the spider peptide toxin lycosin-I through different pathways at different concentrations. It was found that by inactivating STAT3 pathway, high concentrations of lycosin-I induce apoptosis in prostate cancer cells and low concentrations of lycosin-I inhibit the migration of prostate cancer cells. This finding provides favorable evidence for further study of the molecular diversity of spider toxins.

Keywords: Spider peptide toxin lycosin-I, apoptosis, STAT3, MMP9, prostate cancer, tumor

***Experimental Biology and Medicine* 2018; 243: 725–735. DOI: 10.1177/1535370218772802**

Introduction

Prostate cancer (PCA) is a cancer to which men worldwide are predisposed. PCA is a leading cause of cancer-related death in men. Although various methods of treatment have been used to treat local PCA, including prostatectomy, radiotherapy, and androgen deprivation therapy, PCA can eventually progress to be a castration-resistant prostate cancer (CRPC) that has no response to current therapies.

Animal polypeptide toxins, including spider toxins, scorpion toxins, and snake toxins, have become important topics in medical research. The composition of spider venom is complex, including neurotoxic peptide, protein, and other low-molecular weight substances. Most of the spider toxins are polypeptides with three to five disulfide bonds, with specific effects on voltage-gated[1–4] and ligand-gated ion channels,[5–8] with functions of inhibition, blocking, and excitation. Compared with other animal species, spiders, with up to 40,000 species, are the most abundant source of animal toxins.[9] Representative molecules of spider peptide toxins are diverse, and various neurotoxins, kinin analogs, and antimicrobial peptides can be isolated following improvements in isolation and purification techniques. It has been reported in recent years that compounds either isolated from the blood, such as acanthoscrurrin and gomesin, or from spider venoms, such as LyeTx I and lycosin-I, all have strong antibacterial activity. Among these, lycosin-I is a common helical antibacterial peptide isolated from tarantula venom with a hydrophilic α-helical structure.[10] Lycosin-I has antibacterial activity against fungi, Gram-negative bacteria, and Gram-positive bacteria and acts directly on bacterial cell membranes.[11] In addition, lycosin-I can effectively inhibit tumor growth *in vitro*.

For example, 40 μM of lycosin-I is effective against seven cancer cell lines (HeLa, HT1080, H1299, A549, DU145, HCT116, and HepG2) with a lethal rate of 90%, while it has lower toxicity to three normal human tissue cell lines.[11] In three tumor models of mice (A549, HeLa cells, H1299), previous studies have shown that lycosin-I effectively inhibits tumor growth *in vivo* and *in vitro* and induces apoptosis by activating the mitochondrial apoptotic pathway.[12] Recent studies have found that drugs exert a tumor suppressor effect in different ways at different concentrations.[13,14] For example, 1-phosphate calcium uracil (1-CP-U), a synthetic pyrimidine derivative that enhances the body's immune system and regulates renal function, with a variety of pharmacological effects including analgesia and antipyretic effect,[15] induces apoptosis of Hela cells by increasing Bax expression and inhibiting Bcl-2 expression at high concentrations (1.4 μM), whereas it inhibits the expression of MMP2 and MMP9 at low concentrations (0.7 μM), reducing the invasion ability of Hela.[16] Inspired by previous studies, the present study aims to investigate the effects of different concentrations of lycosin-I on the invasiveness and apoptosis of human PCA cells. We found that by inactivating signal transducer and activator of transcription 3 (STAT3) pathway, high concentrations of lycosin-I induce apoptosis in PCA cells and low concentrations of lycosin-I inhibit the migration of PCA cells.

STAT3 is an important member of transcriptional and activation families. The STAT3 signaling pathway is closely related to cell proliferation, differentiation, and apoptosis, leading to abnormal cell proliferation and malignant transformation, which is currently defined as oncogenic. STAT3 has been shown to be overactivated and expressed in many human and murine malignancies including leukemia, multiple myeloma, head and neck squamous cell carcinoma, multiple melanoma, breast, prostate, and lung cancers. The increase of STAT3 to abnormal expression or activity and tumor development is closely related.[17,18] When STAT3 is activated by upstream TAK, p-STAT3 is formed and then p-STAT3 becomes a dimer, which enters the nucleus and regulates the transcriptional activity of the target gene associated with proliferation, differentiation, migration, and other actions of cancer cells. Segatto et al. reported that STAT3 and its activated form of p-STAT3 can promote tumor cell migration and invasion. In PCA cells, STAT3 not only regulates PCA tumor initiating cells[19–21] but also plays an important role in the progression of CRPC.[22,23]

This study shows that lycosin-I exhibits a concentration-dependent mechanism in which lycosin-I induces apoptosis of PCA cells and inhibits cell invasion, specifically inducing apoptosis in PCA cells at high concentration, and inhibiting the migration of PCA cells at low concentrations. Therefore, the determination of a concentration-dependent inhibition mechanism provides a theoretical basis for further clinical application of lycosin-I.

Materials and methods

Experimental reagents and supplies

Hormone-independent hormone PCA PC-3 and DU-145 cell lines (Institute of Cell Research, Shanghai Institute of Chinese Academy of Sciences, Shanghai, China); ECL Developer (GE Healthcare), DMEM high glucose medium (Gibco); other reagents (purchased from Sigma).

Cell culture

DU-145 and PC-3 cell lines were cultured in high glucose DMEM medium supplemented with 10% fetal bovine serum, cultured in a 37°C and 5% CO_2 until the cells cover the bottom of the flask. Cells were passaged for just one time and cultured. The logarithmic growth phase of cells was selected for experimental use. Cell morphology was examined under a light microscope (Zeiss, Axiovert 200, Germany).

Detection of cell activity by MTT

The cells in the logarithmic growth phase were collected, and the concentration of the cell suspension was adjusted. The cells were inoculated into 96-well plates at the number of 1×10^5 cells/well, and the volume of each well was 100 μL. The cells were cultured in a 37°C and 5% CO_2 incubator until the monolayer cells covered the plate bottom, and the experimental groups were then given interventions of 5, 10, and 20 μmol/L lycosin-I for 1 d, 2 d, 3 d, 4 d, 5 d, and 6 d, respectively. The control wells (cells, drug dissolution medium with the same concentration, mediums) and zero-adjustment wells (medium) were set with each group of six complex wells. After each incubation period, 20 μL of fresh 5 g/L MTT was added to each well. After incubation for 4 h, the medium in each well was removed and 150 μL of DMSO was added and the wells were further incubated for 10 min. The absorbance (490 nm) of each well was measured using a Thermo Labsystems 352 Multiskan MS ELISA plate (Labsystems Oy, Helsinki, Finland), and the inhibition of lycosin-1 cells was calculated according to the following formula: Inhibition rate (%) = (1−OD value of the group/OD value of the control group) × 100%. This experiment was repeated three times.

Detection of apoptosis

For DAPI staining, the cells in the logarithmic growth phase were collected and the concentration of cell suspension was adjusted. The cells were inoculated into six wells at 5×10^5 cells per well. The control group and experimental group were set at 37°C and 5% CO_2 in an incubator. After the monolayer covered the bottom of the plate, each experimental group was given an intervention of 5, 10, and 20 μmol/L of lycosin-I for 48 h, respectively. The control group received no intervention. The medium was removed, and culture was washed with phosphate-buffered saline (PBS) two times; DAPI-staining solution (Beyotime) was added away from the light and at room temperature for 15 min; the staining solution was aspirated, and then cells were washed three times in a PBS table concentrator for

5 min each time; the cells were observed under a fluorescence microscope.

Flow cytometry

The cells in the logarithmic growth phase were collected and the concentration of cell suspension was adjusted. The cells were inoculated into six wells at 5×10^5 cells per well. The control group and experimental group were set at 37°C and 5% CO_2 in an incubator. After the monolayer covered the bottom of the plate, the experimental groups were given interventions of 5, 10, and 20 μmol/L lycosin-I for 48 h. The control group received no intervention. Trypsin was used to digest cells, then washed twice with PBS, and then the cells were resuspended in PBS again, stained with 5 μL of LAnnexin V-FITC and 10 μL propidium iodide (PI) in the dark, and the percentage of apoptotic cells was determined by FCM (BD, NJ, USA).

RNA purification and real-time quantitative fluorescent PCR detection

Total RNA was obtained from the cultured cells using the TRIzol reagent method (Invitrogen). Total RNA (1 μg) was reverse transcribed using a PrimeScript RT kit (Takara) to obtain cDNA as a template. Experiments were performed according to the SYBR Premix Ex TaqTM II kit (Takara) operating instructions and quantitative RT-PCR assays were performed on a 7900HT PCR instrument (Applied Biosystems). Three replicate wells were set up, and the relative expression level of mRNA was calculated using the 2-△△ triangle CT method. Primer sequences were as follows: GAPDH (Forward: GGAGCGAGATCCCTCCAAAAT; Reverse: GGCTGTTGTCATACTTCTCATGG); TIMP1 (Forward: ACCACCTTATACCAGCGTTATGA; Reverse: GGTGTAGACGAACCGGATGTC); TIMP2 (Forward: GCTGCGAGTGCAAGATCAC; Reverse: TGGTGCCCGTTGATGTTCTTC); MMP1 (Forward: GAAAGAAGACAAAGGCAAGTTGA; Reverse: CCACATCTGGGCTGCTTCAT); MMP9 (Forward: TGTACCGCTATGGTTACACTCG; Reverse: GGCAGGGACAGTTGCTTCT).

Western blot

The cells in logarithmic growth phase were collected, and the concentration of cell suspension was adjusted. The cells were inoculated into six wells at 5×10^5 cells per well. The control group and experimental group were set at 37°C and 5% CO_2 in an incubator. After the monolayer covered the bottom of the plate, the experimental groups were given interventions of 5, 10, and 20 μmol/L lycosin-I for 48 h. The control group received no intervention. The medium was removed, and the cells washed three times with PBS. RIPA lysate (1 mL) containing protease inhibitor and phosphatase inhibitor was added to each well, and lysed on ice for 10 min. A cell scraper was used to collect cell debris and centrifuged at 12,000*g* for 15 min. The cell supernatants were harvested, and the protein concentration was determined using the BCA method. The protein lysate was placed in a metal bath for degeneration. The loading volume was calculated for each sample protein concentration and electrophoresed on 10% polyacrylamide gel (SDS-PAGE) for 1 h. The separated proteins were electrotransferred to a polyvinylidene fluoride (PVDF) membrane. PVDF was transferred into an incubation box, blocking solution added, and enclosed in a decolorization table at room temperature for 1 h. Anti-STAT3, p-STAT3, MMP9, caspase-9, caspase-3, purchased from Cell signaling Technology, Danvers, MA, USA) and β-actin (Abcam, Cambridge, UK) were incubated. Antibody was diluted to the recommended working concentration, and a PVDF membrane was placed into the antibody solution and incubated on a decolorization table concentrator in a 4°C shaker overnight. After incubation, TBST was rinsed three times for 15 min each. The second antibody was diluted to the appropriate working concentration, according to the instructions, and the PVDF membrane was put into the antibody solution and incubated on a decolorization table concentrator for 1 h. After incubation, TBST was rinsed three times for 15 min each. Immunoreactive protein bands were detected using the ECL kit.

Transwell migration test

Cell migration assays were performed using Matrigel transwell (polycarbonate membrane, 8 μm pore size). Matrigel (0.5 mg/mL) was coated on the upper chamber surface of the bottom membrane of transwell chamber, incubated at 37°C and 5% CO_2 for 30 min to polymerize and coagulate the Matrigel. The tip of a 200 μL pipette tip was cut off and fibronectin was aspirated evenly over the chamber and allowed to air dry at room temperature. Preparation of cell suspension: DU-145 and PC-3 cells were cultured in serum-free fetal bovine serum (FBS)-free DMEM medium for 24 h. Cells were harvested by digestion, washed twice with PBS, and resuspended in BSA-free serum-free medium. The cell density was adjusted and the cell suspension (2×10^6 cells/mL, 100 μL/well) was seeded into the upper chamber of a transwell plate containing 0.1% FBS. In the lower chamber, 600 μL of DMEM containing 20% FBS was added, and the corresponding intervention was given according to the experimental group and the control group. Transwell plates were incubated for 24 h at 37°C in a 5% CO_2 incubator. After incubation, the culture solution was aspirated, and the adherent cells inside the upper chamber polycarbonate membrane were gently wiped with a cotton swab, rinsed twice with PBS, and fixed with 4% paraformaldehyde for 10 min; the fixed solution was aspirated off and the membrane was air-dried, and then 0.1% crystal violet dye was added into the wells and allowed to stand at room temperature for 20 min. The staining solution was gently shaken off, the wells washed with deionized water, the upper chamber was removed, the interior of the polycarbonate membrane was gently blotted with a filter paper, the upper chamber of the experimental group was placed into the new 24-well plate, decolored with 33% acetic acid; each well was filled with 100 μL of decolorizing solution in a 96-well plate, with each group of five complex wells; at the same time, the zero-adjustment

wells (33% acetic acid) were set and the OD 490 nm away from the ELISA was detected.

Cell scratch test

Before the inoculation of cells, a line was first drawn evenly behind the six-well plate with a marker pen. The cells were seeded in six-well plates at a density of 5×10^3 cells/well, and the experimental groups were intervened with 5 μmol/L lycosin-I and the control groups were 0 μmol/L lycosin-I. When the bottom of the wells was covered by cells, tips were used to draw a trace to form a bare area. The cells were washed three times with PBS, and then serum-free medium was added. Cells were placed in 37°C, 5% CO_2 incubator for 24 h. Under a light microscope, the distance of migration of the cells to the scratch area was measured at 100-fold magnification. This experimental method can determine the invasiveness of PCA cells. Five different migration points for each sample were chosen and the distance and average were measured.

Xenografts to construct tumor models

The experiment obtained approval for animal studies by the research ethics committee of the second Xiangya Hospital, Central South University. Female sterile eight-week-old BALB/c nude mice were purchased from Changsha Shakespeare Experimental Animal Company and housed in a specific pathogen free (SPF) animal room. The nude mice were fed on sterilized feed specially formulated for mice, free to drink sterile water, and the animal laboratory temperature was maintained at 20–25°C, relative humidity maintained at 50–70%. To test the effect of lycosin-I in mice, logarithmic growth phase human prostate cell line PC-3 and DU-145 cells were collected, and cells were resuspended in PBS to prepare a cell suspension at a concentration of 2×10^7/mL. A 1 mL syringe needle was used to gently tap the skin of the right shoulder of the nude mouse and a 0.2 mL cell suspension was injected subcutaneously to form a subcutaneous hillock. After the tumor diameter reached about 5–6 mm, 50, 100, or 200 μg of lycosin-1 was dissolved in 100 μL of saline to prepare different concentrations of the drug to be used, and for the experimental group and control group, 100 μL of drug or equivalent volume of saline was injected into the tumor. On the 28th day after the first treatment, 40 mice were euthanized to obtain a tumor for use.

Immunohistochemistry

The xenografted tumor tissue was fixed for 24 h and embedded in paraffin to make 4 μm paraffin sections. Paraffin sections were placed in an oven at 67°C for 1 h;

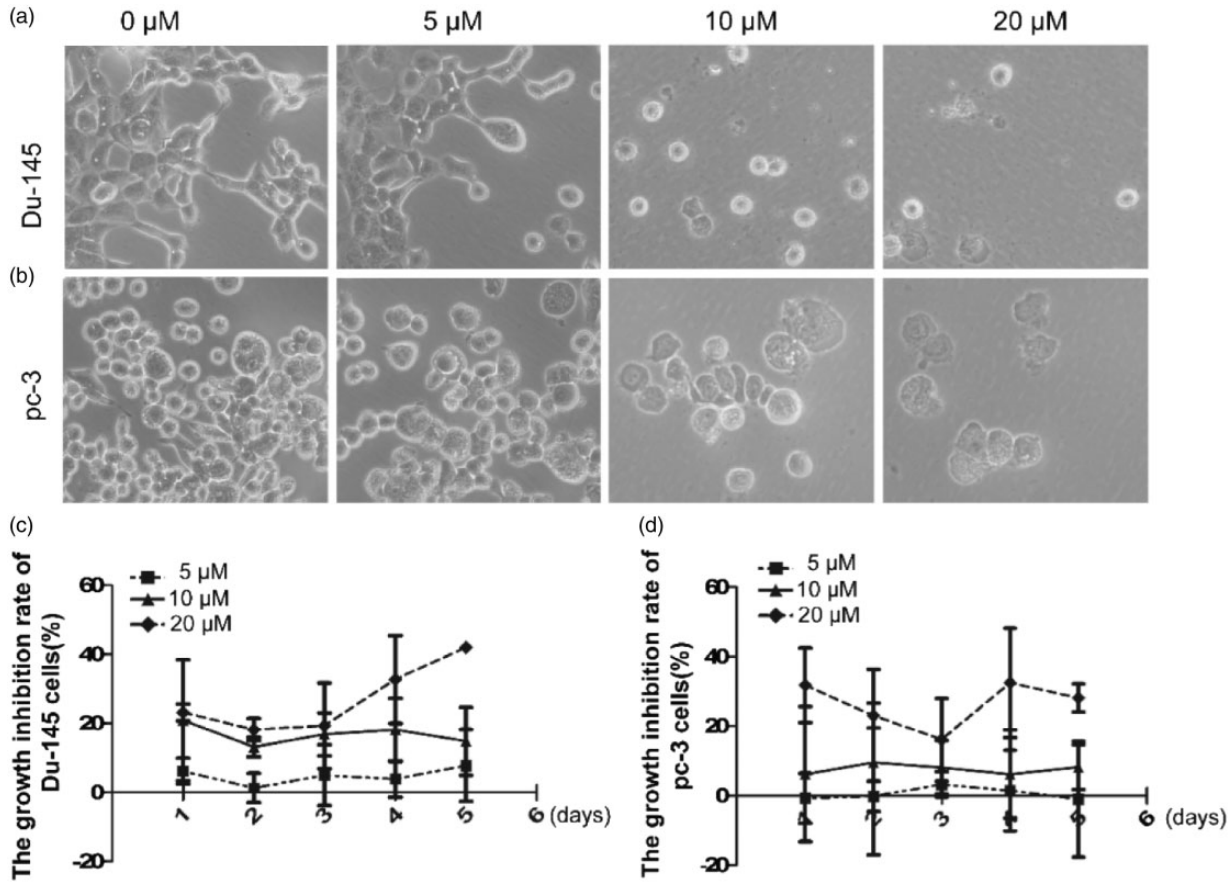

Figure 1. Lycosin-I caused morphological changes in cells and inhibited cell proliferation. The effect of lycosin-I at different concentrations (5 μM, 10 μM, and 20 μM) on the growth morphology of PCA, DU-145, and PC-3 cells (a and b). The effects of different concentrations of lycosin-I on the growth inhibition of prostate cancer cells were detected by MTT assay (c, d) (Student's t-test, $P_1 > 0.05$, $P_2 < 0.05$, $P_3 < 0.01$).

xylene II was added for 10 min, and gradient alcohol with concentrations of 100% for 2 min, 95% for 2 min, 80% for 2 min, 70% for 2 min was added. Paraffin sections were rinsed two times with PBS (placed in the table concentrator), 3 min each time, dewaxed and water treatment was performed. A certain amount of citrate buffer pH = 6.0 was added to the microwave box, heated to boiling (about 95°C), and then the dewaxed hydration of tissue slice was placed in a plastic slice rack of high temperature resistance, put into the boiling buffer for 20 min for antigen recovery. Slides were removed, rinsed two times with PBS, 3 min each time (placed in the table concentrator); one drop of 3% H_2O_2 was added to each slice, and slices were incubated for 20 min at room temperature to block endogenous peroxidase activity; rinsed two times with PBS, 3 min each time (placed in the table concentrator); slices were sealed in 5% BSA at 37°C for 20 min; 100 μL of antibody specific to human STAT3 and p-STAT3 (1:100 dilution; R & D Systems) and rabbit monoclonal antibody specific to MMP9 (1:100 dilution(1 d 100 μL of a specific antibody to human STago, IL) were added on the slices (covering tissues); slices were incubated at 4°C overnight, rinsed two times with PBS, 3 min each time (placed in the table concentrator); diluted biotinylated secondary antibody was added to the slices

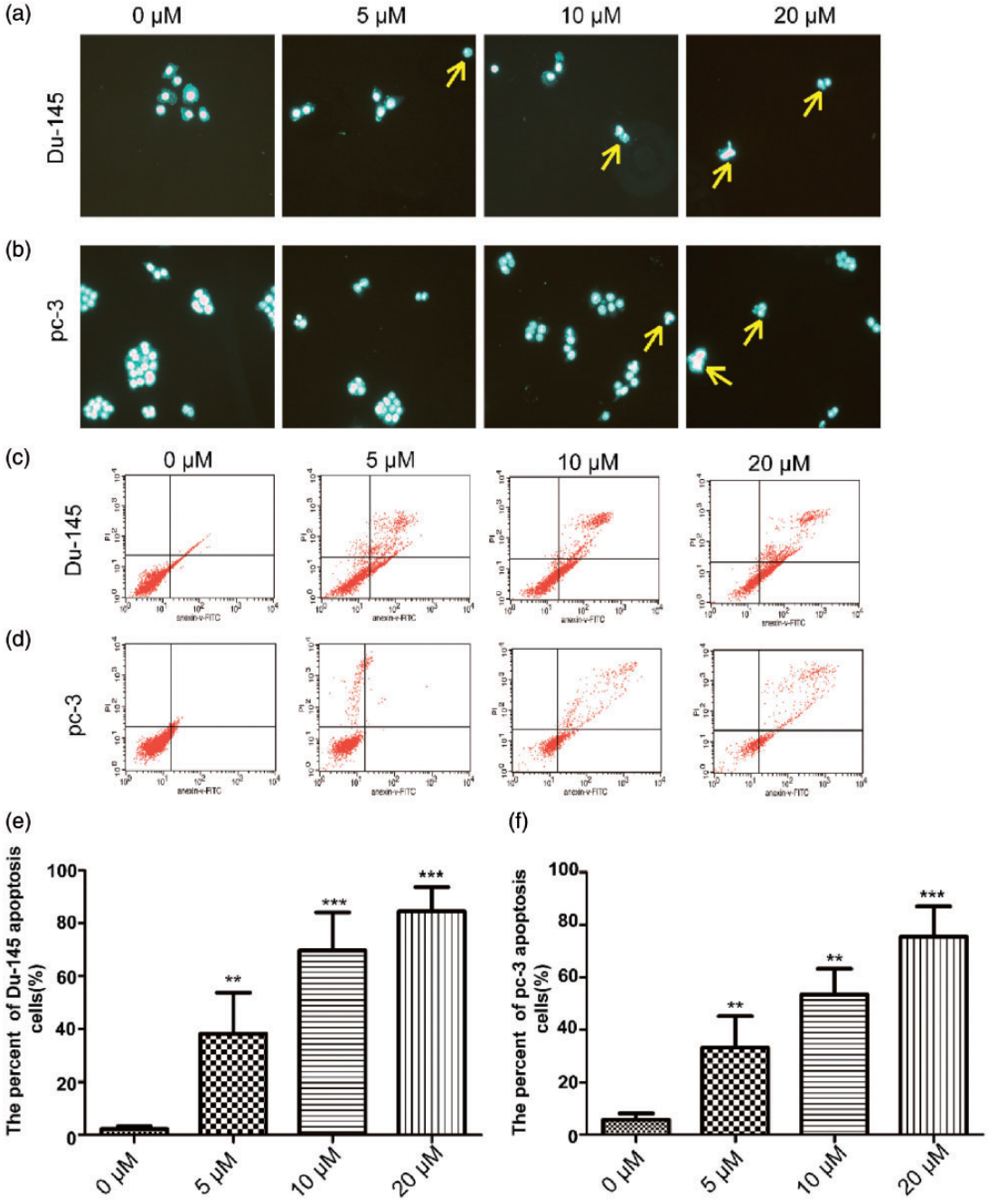

Figure 2. Lycosin-I at high concentrations promoted apoptosis of prostate cancer cells. DAPI staining was performed on PCA, DU-145, and PC-3 cells that had been induced to apoptosis by lycosin-I (a, b); FCM analysis was performed on PCA, DU-145, and PC-3 cells that had been induced to apoptosis by lycosin-I (c, d); when treated with different concentrations of lycosin-I, the apoptotic rates of PCA, DU-145, and PC-3 cells (e, F) (Student's t-test, $P_1>0.05$, $P_2<0.01$, $P_3<0.01$).

and slices were incubated at 37°C for 20 min. Fresh 3,3-diaminophenylethyridine (DAB) solution was used for color development and slices were observed under the microscope, and timely stopped.

TUNEL staining

Paraffin sections were placed in an oven at 67°C for 1 h; xylene II was added for 10 min, and gradient alcohol with concentrations of 100% for 2 min, 95% for 2 min, 80% for 2 min, 70% for 2 min was added. Paraffin sections were rinsed two times with PBS (place in the table concentrator), 3 min each time, dewaxed and performed water treatment; One drop of 3% H_2O_2 was added in each slice, and slices were incubated for 20 min at room temperature to block the endogenous peroxidase activity, rinsed two times with PBS (place in the table concentrator), 3 min each time; slices were performed according to the operating instructions of the TUNEL staining (TUNEL Kit, Boehringer, Mannheim) kit: Protease K (dissolve 20 μg/mL in Tris/HCl, pH 7.4 to 8.0) was added for 30 min at room temperature; manufacturer's instructions were followed with minor modifications: digested by protease K 20 μg/mL for 30 min at 37°C, rinsed two times with PBS, 3 min each time (place in the table concentrator); in accordance with the operating instructions, the TUNEL reaction mixture solutions were configured (i.e. ready-to-use, away from light), i.e. TdT and dUTP mixtures, 50 μL of the reaction solution was added onto the slices, and slices were incubated at 37°C for 60 min, rinsed two times with PBS, 3 min each time; the moisture around the sample was dried and 50 μL of the transforming reagent-POD was added; slices were incubated in a humid chamber at 37°C for 30 min and rinsed two times with PBS, 3 min each time; freshly prepared diaminobenzidine (DAB) reagent was added, and slices were incubated for 5 min at room temperature, rinsed two times with PBS, 3 min each time. Slices were placed on a glass slide to observe the results.

Statistical analysis

Statistical analysis was performed using SPSS 17.0 and the data are presented as mean ± SD. Dunnett's multiple comparison test was performed using analysis of variance (ANOVA) to compare two groups or more. Student's t-test was used to compare the differences between the two groups. $P < 0.05$ for the difference was taken to be statistically significant.

Results

Lycosin-I caused morphological changes in cells and inhibited cell proliferation in a dose-dependent manner

To investigate the cytotoxic effect of lycosin-I on DU-145 and PC-3 cells, we observed the morphological and

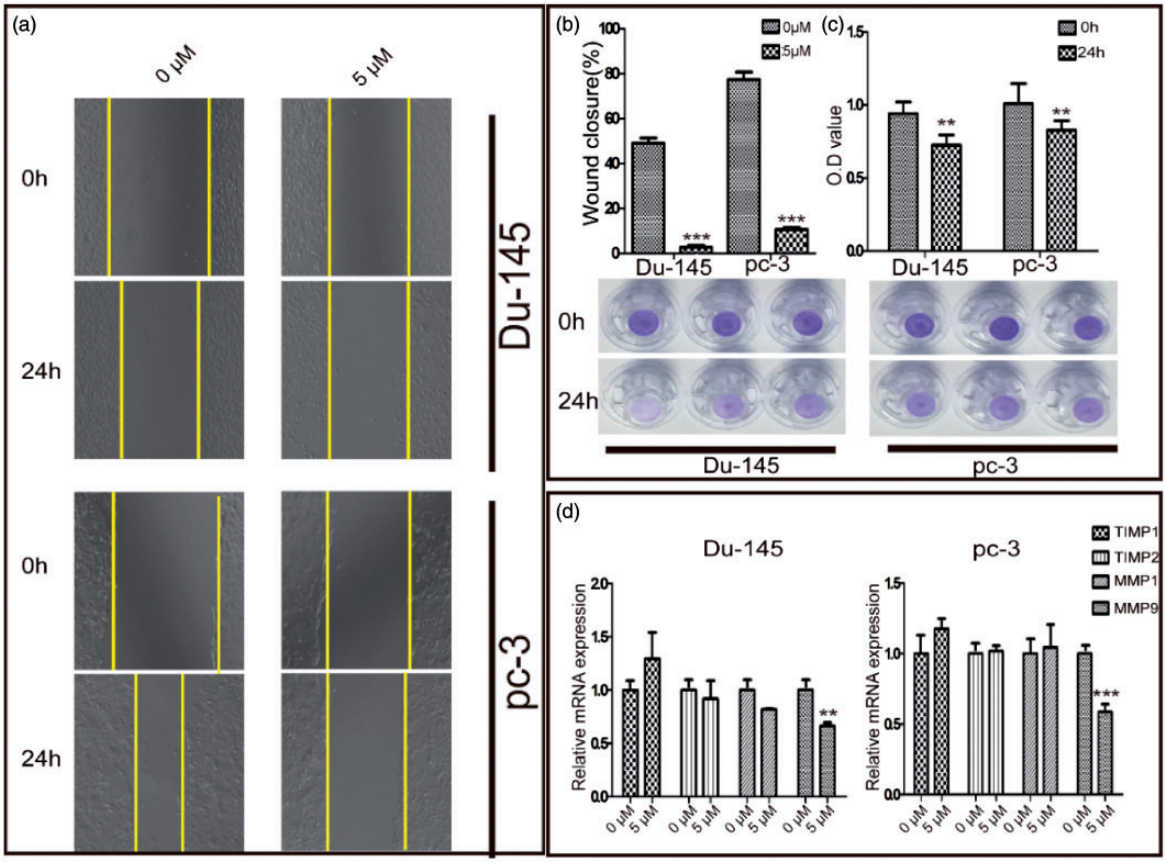

Figure 3. Lycosin-I with low concentration inhibited DU145 and PC-3 migration. Scratch test: The effect of different concentrations of lycosin-I on the invasiveness of DU-145 and PC-3 cells was evaluated by cell scratch assay (a) (Student's t-test, $P < 0.01$). Transwell assay. The effect of 5 μM of lycosin-1 treatment on the migration ability of DU-145 and PC-3 prostate cancer cells was detected, 24 h OD values were recorded (b) (Student's t-test, $P < 0.01$). mRNA expression levels of TIMP1, TIMP2, MMP1, MMP9 of DU-145 and PC-3, when treated with 5 μM of lycosin-I (c).

biochemical changes of lycosin-I-treated cells at various concentrations. Microscopy showed that as the concentration of lycosin-I increased, the morphological changes of the cells became more and more significant. As shown in Figure 1(a), DU-145 and PC-3 cells grew normally with normal spindle or oval form, and with intact cell membranes when cultured in medium without lycosin-1. When treated with lycosin-I for 24 h, there was no significant change in the cell morphology of DU145 and PC-3 cells treated with 5 μM of lycosin-1 compared with the control group. However, DU145 and PC-3 cells shrank, and shrank into a circle, when the lycosin-I levels increased to 10 μM and 20 μM, respectively.

In addition, to further confirm the inhibitory effect of lycosin-I on cell proliferation *in vitro*, an MTT assay was performed. The results showed that 5 μM lycosin-I tumor cells in both groups showed no significant cytotoxicity, while lycosin-1 at 10 μm and 20 μM significantly inhibited cell proliferation, and the inhibitory effect of lycosin-I was significantly dose dependent.

Lycosin-I at high concentrations promoted apoptosis of PCA cells

To investigate the cytotoxic effect of lycosin-I, the interfering cells were stained with DAPI. The results, observed with a fluorescence microscope, showed that the cells had intact nuclear and chromatin staining uniformity in the control group of DU-145 and PC-3 cells. Meanwhile, in those groups that were treated with 5 μM of lycosin-I, there was also no significant change in the morphology and staining of nuclei in these cells. Some events of karyopyknosis and chromatin deep dyeing were observed in 10 μM of lycosin-I-treated cells with occurrence of apoptosis body (shown by the yellow arrow in Figure 2(a)). Some of the cells in the 20 μM of lycosin-I-treated cells had no intact nuclei, or were fragmented into fragments of different sizes (Figure 2(b), shown by yellow arrow). Subsequent Annexin V-FITC/PI fluorescence staining showed that there was no significant apoptosis of DU-145 and PC-3 cells treated with 5 μM of lycosin-I compared with the control group (DU-145: 0 μM: 2.20 ± 1.83%, 5 μM: 8.22 ± 3.78%, PC-3: 0 μM: 5.59 ± 4.38%, 5 μM: 12.15 ± 5.89%). When the lycosin-I dose increased to 10 μM and 20 μM, the number of apoptotic DU-145 and PC-3 cells gradually increased with the increase of lycosin-I dose (DU-145: 10 μM: 69.67 ± 24.90%, 20 μM: 84.45 ± 15.86%; PC-3: 10 μM: 53.45 ± 17.12%, 20 μM: 75.43 ± 19.91%) (Figure 2(c) to (f)). The results showed that low concentrations of lycosin-1 had no obvious cytotoxic effect on DU-145 and PC-3 cells. However, when lycosin-I concentration reached 10 μM, it induced an increase in the number of apoptotic cells with increasing concentration.

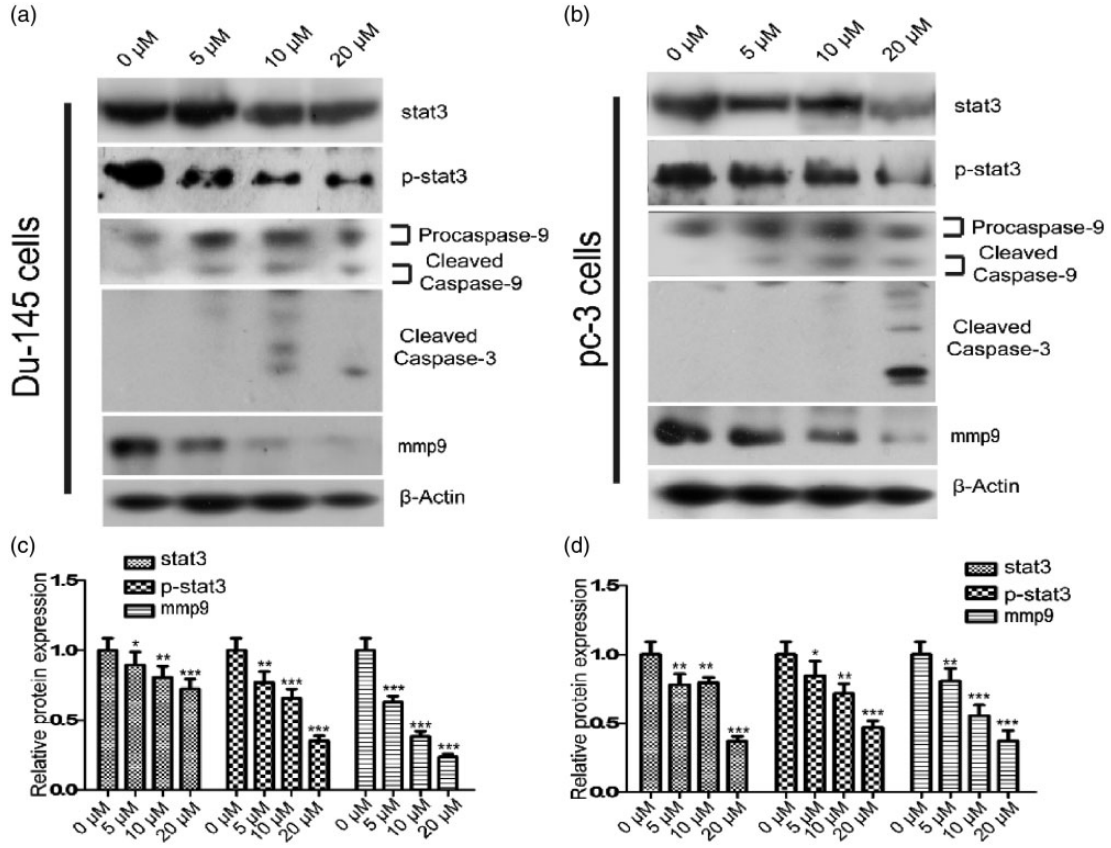

Figure 4. Lycosin-I prevented DU145 and PC-3 cells through inactivated STAT3 pathway. Western blot analysis. The level of expression to STAT3, p-STAT3, caspase-9, cleaved caspase-9, cleaved caspase-3, and MMP9 were detected in DU-145 and PC-3 cells after treatment with different concentrations of lycosin-I. Analysis of protein expression of STAT3, p-STAT3, and MMP9 (c, d) (ANOVA, $P < 0.05$).

Lycosin-I with low concentrations inhibited DU145 and PC-3 migration

In recent years, different concentrations of drugs have been reported to play different roles.[22] Although lycosin-I at a low concentration has no obvious cytotoxic effects on DU-145 and PC-3, the following experiments demonstrated that low concentrations of lycosin-I inhibited the ability of PCA cells to invade. As shown in Figure 3(a), scratch experiments demonstrated that cells in both control groups entered the scratch space after 24 h. However, the cells treated with 5 μM of lycosin-I showed significantly reduced invasiveness, with a significantly reduced mobility ratio compared with the control group (DU-145: $3.32 \pm 1.63\%$ vs. $18.32 \pm 2.68\%$, PC-3: $6.78 \pm 2.72\%$ vs. $48.67 \pm 6.73\%$), indicating that lycosin-I significantly inhibited the invasiveness of DU-145 and PC-3 cells (Figure 3(a) and (b)). The results of a transwell assay showed that the membrane staining of the experimental group was weaker than that of the control group after being treated with 5 μM of lycosin-1 (Figure 3(c) and (d)), further confirming that 5 μM of lycosin-1 significantly inhibited the migration ability of DU-145 and PC-3 cells. Next, we used real-time PCR to detect changes in gene expression associated with tumor invasion and metastasis. It was found that mRNA expression of MMP9 was significantly decreased in DU-145 and PC-3 cells when treated with 5 μM of lycosin-I, while there was no significant change in other tumor invasion and metastasis genes TIMP1, TIMP2, TIMP3, and MMP1 (Figure 3(d)). This shows that lycosin-I could inhibit the cell migration by down-regulating the expression of MMP9.

Lycosin-I promoted apoptosis and inhibited cell migration in DU145 and PC-3 cells through inactivated STAT3 pathway

To clarify the mechanism of lycosin-I promoting apoptosis and inhibiting migration in DU145 and PC-3 cells, we examined the expressions of STAT3 and p-STAT3, caspase-3, caspase-9, and after RT-PCR verification, there was a changed expression for invading the related protein MMP9 and found that the expression of STAT3 and p-STAT3 gradually decreased with the increase of lycosin-I concentration. When treated with a low concentration of lycosin-I, the cleaved caspase-9 expression was increased compared with the control group, but the expression of cleaved caspase-3 did not change significantly. However, in the case of a high concentration of lycosin-I, the expression of cleaved caspase-3 and cleaved caspase-9 increased and showed a dose-dependent increase. The highest concentrations of these proteins were detected in cells treated with 20 μM of lycosin-I, indicating that lycosin-1 could activate apoptotic signaling and promote apoptosis of DU-145, PC-3, and PCA cells at high concentrations (Figure 4(a) and (b)). We also studied the expression of MMP9, a protein involved in invasion and migration, and found that the expression of this protein decreased with decreasing concentration (Figure 4(c) and (d)). These results show that lycosin-I could inhibit the migration of PC-3 and DU-145 through the inactivated STAT3 pathway and promote the apoptosis of PC-3 and DU-145.

Lycosin-I inhibited proliferation of PC-3 and DU-145 in nude mouse models

To investigate the inhibitory effect of lycosin-I on DU-145 and PC-3 *in vivo*, we subcutaneously injected 50 μg, 100 μg, and 200 μg of lycosin-I into nude mice bearing tumors injected with PC-3 or DU-145 and monitored the tumor growth for more than four weeks. All tumors in the PC-3 and DU-145 experimental groups were found to be smaller than the control group (DU-145: 50 μg: 10.02 ± 2.40 mm, 100 μg: 8.15 ± 0.99 mm, 200 μg: 5.15 ± 1.04 mm vs. 0 μg: 10.35 ± 3.28 mm, PC-3: 50 μg: 11.82 ± 1.42 mm, 100 μg: 8.67 ± 0.50 mm, 200 μg: 6.76 ± 0.40 mm, 0 μg: 12.11 ± 1.70 mm). Interestingly, the tumor diameter of both PC-3 and DU-145 tumor cells was significantly reduced with increasing lycosin-I concentration. As shown in Figure 5(a) and (b), lycosin-I could inhibit the growth of implanted DU-145 and PC-3 tumors in a dose-dependent manner. Next, to understand how lycosin-I inhibits the proliferation of PC-3 and DU-145, we performed tumor tissue immunohistochemistry and TUNEL staining of STAT3, p-STAT3, and MMP9 (Figures 6(a) to (d) and 7(a to d)). As shown in Figures 6 (a) to (d) and 7(a) to (d), the staining intensity of STAT3,

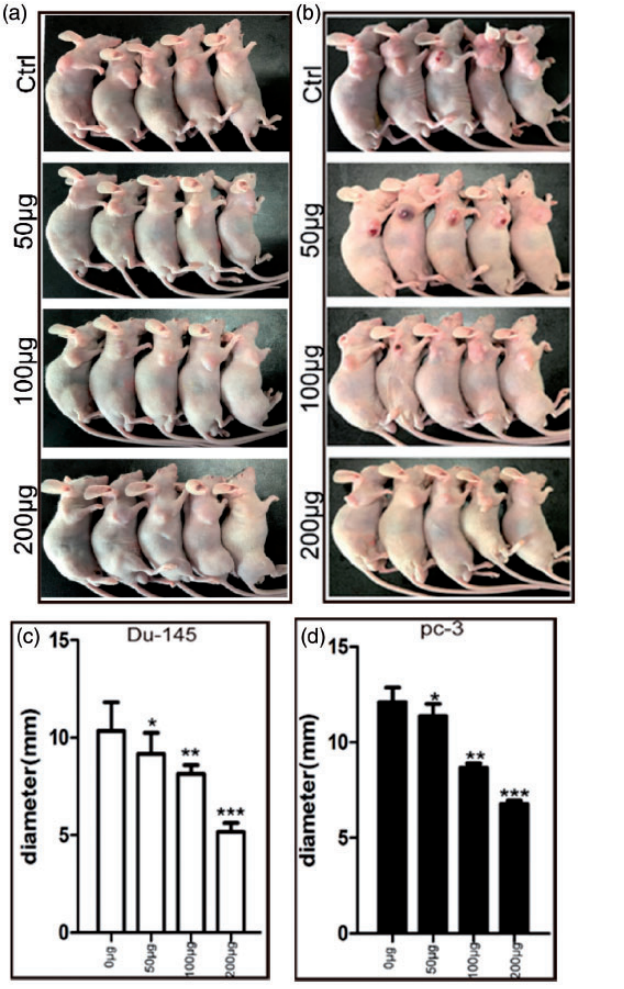

Figure 5. Lycosin-I inhibited proliferation of PC-3 and DU-145 in nude mouse models. The effect of different concentrations of lycosin-I (control group, 50 μg, 100 μg, and 200 μg) on tumor growth (a, b) and tumor diameter (c, d) of DU-145 and PC-3 *in vivo* (ANOVA, $P < 0.05$).

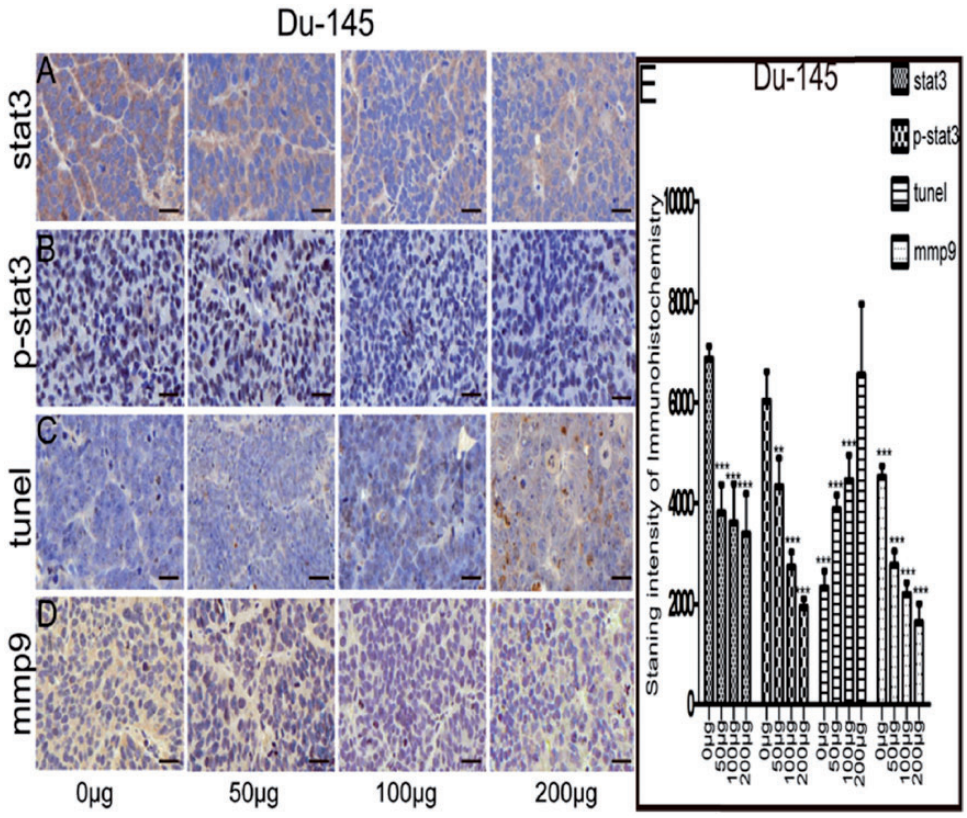

Figure 6. Lycosin-I inhibited proliferation of DU-145 in nude mouse models. Representative images (a, b, c, d) of STAT3, p-STAT3, TUNEL, and MMP9 in DU-145 prostate cancer cells detected in different concentrations of lycosin-I (control, 50 μg, 100 μg, and 200 μg). Immunohistochemical staining intensity (e) of STAT3, p-STAT3, TUNEL, and MMP9 after treatment of different concentrations of lycosin-I (control, 50 μg, 100 μg, and 200 μg) (ANOVA, $P < 0.05$).

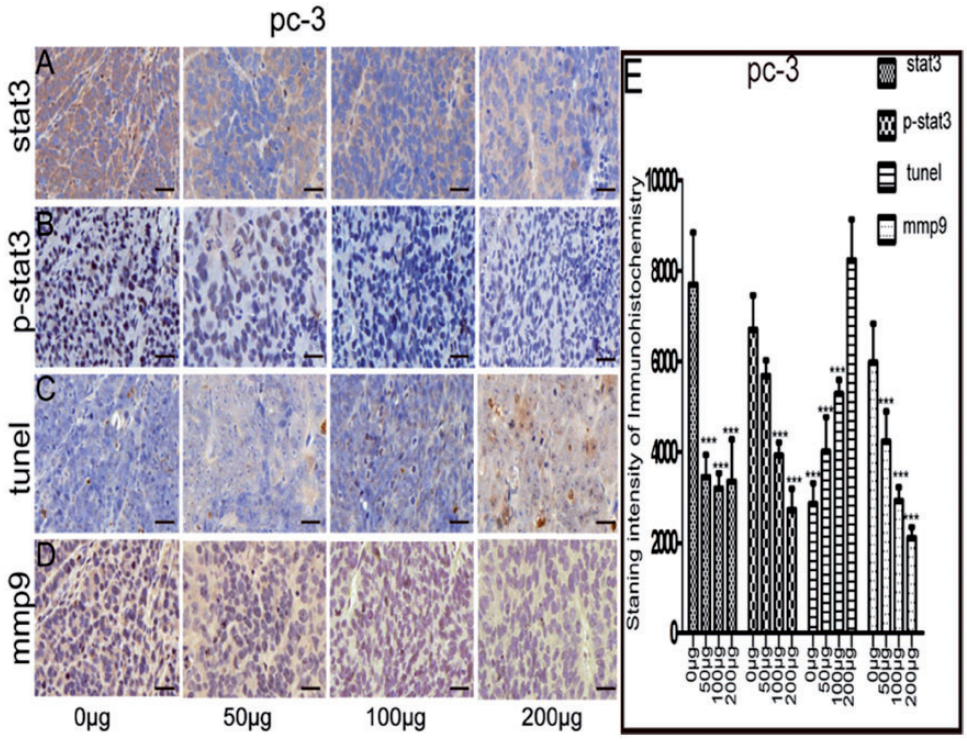

Figure 7. Lycosin-I-inhibited proliferation of PC-3 in nude mouse models. Representative images (a, b, c, d) of STAT3, p-STAT3, TUNEL, and MMP9 in PC-3 prostate cancer cells detected in different concentrations of lycosin-I (control, 50 μg, 100 μg, and 200 μg). Immunohistochemical staining intensity (e) of STAT3, p-STAT3, TUNEL, and MMP9 after treatment of different concentrations of lycosin-I (control, 50 μg, 100 μg, and 200 μg) (ANOVA, $P < 0.05$).

p-STAT3, and MMP9 in DU-145 and PC-3 cells gradually decreased with the increase of lycosin-I concentration. However, compared with the control group, there was no significant change in the staining intensity of the TUNEL treated with low concentration, and the staining intensity of the TUNEL increased gradually with the increase of the concentration of the TUNEL under the high concentration (>100 μg). This indicated that a low concentration of lycosin-I could not induce tumor cell apoptosis, but could inhibit the migration of PC-3 and DU-145. This demonstrates that low concentrations of lycosin-I significantly inhibited the invasion and metastasis of PC-3 and DU-14 in the absence of apoptosis of tumor cells. High concentrations of lycosin-I could induce apoptosis and inhibit cell migration *in vivo* through the inactivated STAT3 signaling pathway.

Discussion

The incidence of PCA is higher in Western countries than in China.[24,25] However, the morbidity and mortality of PCA are significantly increased in China due to the changes in environment and diet as well as ageing population.[26] Although the incidence in China is still low, the diagnosis of PCA is often at an advanced stage with a low survival rate. In particular, in about 13% to 72% of patients, PCA migrates to the bone marrow early in the disease and metastatic PCA cells remain dormant in metastatic organs for up to 10 years.[19] Therefore, the treatment goals of prostate cancer drugs are not only to induce the apoptosis of PCA cells but also to inhibit their early invasion and metastasis.

Spider peptide toxins have become an important topic in medical research due to their therapeutic potential. Current studies have found that lycosin-I, a peptide toxin isolated from cryptotanneus venom, not only has antimicrobial activity against bacteria and fungi but also induces apoptosis in cancer cells.[27]

However, our studies found that different concentrations of lycosin-I had different effects on tumors, and that low concentrations (5 μM) of lycosin-1 significantly inhibited PC-3 and DU-145 cell invasion and metastasis in the absence of tumor cell apoptosis. Higher doses of lycosin-I (10 μM, 20 μM) caused morphological changes in PC-3 and DU-145 cells. The gaps between cells increased, cells shrank, and fixation of nuclear chromatin, with the formation of apoptotic bodies, and nuclear lysis was observed. Our studies have found that both STAT3 and phosphorylated STAT3 decreased and MMP9 expression decreased at low concentrations of PC-3 and DU-145 cells treated by lycosin-1, indicating that lycosin-1 MMP9 expression can be inhibited through the STAT3 signaling pathway to inhibit CRPC cells. In addition, in a mouse xenograft model of PCA, immunohistochemistry showed that lycosin-I can promote apoptosis in PC-3 and DU-145 cells and inhibit cell invasion through inactivation of the STAT signaling pathway.

The sustained activation of STAT3 has been found in many solid malignancies of tumors, including musculoskeletal tumors such as Ewing's sarcoma and osteosarcoma.[14,28–30] Therefore, various factors leading to the inactivation of the STAT3 signaling pathway in tumors to promote tumor cell apoptosis and inhibit tumor cell invasion and metastasis have been considered as a method for the treatment of cancer.

The metastasis of a tumor is a complex process in which cells undergo a phenotypic change and migrate from primary tumors, survive in the vasculature, or lymph vessels, and settle in the transfer site. MMPs involved in this process can degrade almost all components of ECM and BM closely related to tumor cell metastasis and tumor angiogenesis.[29] This plays an important role in tumor invasion and metastasis, and previous studies have found that MMP9 and MMP2 are regulated by STAT3.[30]

In general, by inactivating STAT3 pathway, high concentrations of lycosin-I induce apoptosis in PCA cells and low concentrations of lycosin-I inhibit the migration of PCA cells. This finding provides favorable evidence for further study of the molecular diversity of spider toxins. In our opinion, with the further development of purification technology and the mechanism of spider toxin activity, the clinical application of lycosin-I will further expand the research and provide a new method for the clinical treatment of tumors.

Author contributions: LY and HS conceived and designed the experiments; HS, YX, and SY performed the experiments; HS analyzed the data; HS, SY, RC, and KH wrote the manuscript.

ACKNOWLEDGEMENTS

We thank the Institute of Cell Research, Shanghai Institute of Chinese Academy of Sciences for providing cell lines and the second Xiangya Hospital of Central South University for providing nude mice. The expert technical assistance of Paitao, Zeng and Zheng Wu is gratefully acknowledged.

DECLARATION OF CONFLICTING INTERESTS

The author(s) declared no potential conflicts of interest with respect to the research, authorship, and/or publication of this article.

FUNDING

The author(s) received no financial support for the research, authorship, and/or publication of this article.

REFERENCES

1. Lee HC, Wang JM, Swartz KJ. Interaction between extracellular hanatoxin and the resting conformation of the voltage-sensor paddle in Kv channels. *Neuron* 2003;**40**:527–36
2. Lee SY, MacKinnon R. A membrane-access mechanism of ion channel inhibition by voltage sensor toxins from spider venom. *Nature* 2004;**430**:232–5
3. Mintz IM, Venema VJ, Swiderek KM, Lee TD, Bean BP, Adams ME. P-type calcium channels blocked by the spider toxin omega-Aga-IVA. *Nature* 1992;**355**:827–9
4. Phillips LR, Milescu M, Li-Smerin Y, Mindell JA, Kim JI, Swartz KJ. Voltage-sensor activation with a tarantula toxin as cargo. *Nature* 2005;**436**:857–60

5. Bohlen CJ, Priel A, Zhou S, King D, Siemens J, Julius D. A bivalent tarantula toxin activates the capsaicin receptor, TRPV1, by targeting the outer pore domain. *Cell* 2010;**141**:834–45
6. Escoubas P, De Weille JR, Lecoq A, Diochot S, Waldmann R, Champigny G, Moinier D, Menez A, Lazdunski M. Isolation of a tarantula toxin specific for a class of proton-gated Na+ channels. *J Biol Chem* 2000;**275**:25116–21
7. Pinheiro AC, da Silva AJ, Prado MA, Cordeiro Mdo N, Richardson M, Batista MC, de Castro Junior CJ, Massensini AR, Guatimosim C, Romano-Silva MA, Kushmerick C, Gomez MV. Phoneutria spider toxins block ischemia-induced glutamate release, neuronal death, and loss of neurotransmission in hippocampus. *Hippocampus* 2009;**19**:1123–9
8. Siemens J, Zhou S, Piskorowski R, Nikai T, Lumpkin EA, Basbaum AI, King D, Julius D. Spider toxins activate the capsaicin receptor to produce inflammatory pain. *Nature* 2006;**444**:208–12
9. King GF, Hardy MC. Spider-venom peptides: structure, pharmacology, and potential for control of insect pests. *Annu Rev Entomol* 2013;**58**:475–96
10. Tan H, Luo W, Wei L, Chen B, Li W, Xiao L, Manzhos S, Liu Z, Liang S. Quantifying the distribution of the stoichiometric composition of anticancer peptide lycosin-I on the lipid membrane with single molecule spectroscopy. *J Phys Chem B* 2016;**120**:3081–8
11. Tan H, Ding X, Meng S, Liu C, Wang H, Xia L, Liu Z, Liang S. Antimicrobial potential of lycosin-I, a cationic and amphiphilic peptide from the venom of the spider Lycosa singorensis. *CMM* 2013;**13**:900–10
12. Liu Z, Deng M, Xiang J, Ma H, Hu W, Zhao Y, Li DW, Liang S. A novel spider peptide toxin suppresses tumor growth through dual signaling pathways. *CMM* 2012;**12**:1350–60
13. Li J, Zhao YF, Zhao XL, Yuan XY, Gong P. Synthesis and anti-tumor activities of novel pyrazolo[1,5-a]pyrimidines. *Arch Pharm Chem Life Sci* 2006;**339**:593–7
14. Manetti F, Brullo C, Magnani M, Mosci F, Chelli B, Crespan E, Schenone S, Naldini A, Bruno O, Trincavelli ML, Maga G, Carraro F, Martini C, Bondavalli F, Botta M. Structure-based optimization of pyrazolo[3,4-d] pyrimidines as Abl inhibitors and antiproliferative agents toward human leukemia cell lines. *J Med Chem* 2008;**51**:1252–9
15. Peng J, Chen X, Hu Q, Yang M, Liu H, Wei W, Liu S, Wang H. 1calcium phosphateuracil, a synthesized pyrimidine derivative agent, has antiproliferative, proapoptotic and antiinvasion effects on multiple tumor cell lines. *Mol Med Rep* 2014;**10**:2271–8
16. Curran S, Murray GI. Matrix metalloproteinases in tumour invasion and metastasis. *J Pathol* 1999;**189**:300–8
17. Smithgall TE, Briggs SD, Schreiner S, Lerner EC, Cheng H, Wilson MB. Control of myeloid differentiation and survival by Stats. *Oncogene* 2000;**19**:2612–8
18. Rawlings JS, Rosler KM, Harrison DA. The JAK/STAT signaling pathway. *J Cell Sci* 2004;**117**:1281–3
19. Ni Z, Lou W, Leman ES, Gao AC. Inhibition of constitutively activated Stat3 signaling pathway suppresses growth of prostate cancer cells. *Cancer Res* 2000;**60**:1225–8
20. Barton BE, Karras JG, Murphy TF, Barton A, Huang HF. Signal transducer and activator of transcription 3 (STAT3) activation in prostate cancer: direct STAT3 inhibition induces apoptosis in prostate cancer lines. *Mol Cancer Therap* 2004;**3**:11–20
21. Han Z, Wang X, Ma L, Chen L, Xiao M, Huang L, Cao Y, Bai J, Ma D, Zhou J, Hong Z. Inhibition of STAT3 signaling targets both tumor-initiating and differentiated cell populations in prostate cancer. *Oncotarget* 2014;**5**:8416–28
22. Mora LB, Buettner R, Seigne J, Diaz J, Ahmad N, Garcia R, Bowman T, Falcone R, Fairclough R, Cantor A, Muro-Cacho C, Livingston S, Karras J, Pow-Sang J, Jove R. Constitutive activation of Stat3 in human prostate tumors and cell lines: direct inhibition of Stat3 signaling induces apoptosis of prostate cancer cells. *Cancer Res* 2002;**62**:6659–66
23. Abdulghani J, Gu L, Dagvadorj A, Lutz J, Leiby B, Bonuccelli G, Lisanti MP, Zellweger T, Alanen K, Mirtti T, Visakorpi T, Bubendorf L, Nevalainen MT. Stat3 promotes metastatic progression of prostate cancer. *Am J Pathol* 2008;**172**:1717–28
24. Torre LA, Bray F, Siegel RL, Ferlay J, Lortet-Tieulent J, Jemal A. Global cancer statistics, 2012. *CA* 2015;**65**:87–108
25. Center MM, Jemal A, Lortettieulent J, Ward E, Ferlay J, Brawley O, Bray F. International variation in prostate cancer incidence and mortality rates. *Eur Urol* 2012;**61**:1079
26. Chen W, Zheng R, Baade PD, Zhang S, Zeng H, Bray F, Jemal A, Yu XQ, He J. Cancer statistics in China, 2015. *CA* 2016;**66**:115
27. Tan H, Huang Y, Xu J, Chen B, Zhang P, Ye Z, Liang S, Xiao L, Liu Z. Spider toxin peptide lycosin-I functionalized gold nanoparticles for in vivo tumor targeting and therapy. *Theranostics* 2017;**7**:3168–78
28. Wang Y, Chu Y, Yue B, Ma X, Zhang G, Xiang H, Liu Y, Wang T, Wu X, Chen B. Adipose-derived mesenchymal stem cells promote osteosarcoma proliferation and metastasis by activating the STAT3 pathway. *Oncotarget* 2017;**8**:23803–16
29. Sang QX. Complex role of matrix metalloproteinases in angiogenesis. *Cell Res* 1998;**8**:171–7
30. Xie TX, Wei D, Liu M, Gao AC, Ali-Osman F, Sawaya R, Huang S. Stat3 activation regulates the expression of matrix metalloproteinase-2 and tumor invasion and metastasis. *Oncogene* 2004;**23**:3550–60

(Received January 5, 2018, Accepted March 29, 2018)